Microbial Sensing by Goblet Cells Controls Immune Surveillance of Luminal Antigens in the Colon

Kathryn A Knoop[1], **Keely G. McDonald**[1], **Stephanie McCrate**[1], **Jeremiah R McDole**[2], and **Rodney D Newberry**[1,*]

[1]Department of Internal Medicine, Washington University School of Medicine, St. Louis, Missouri, USA, 63110

[2]Department of Pathology and Immunology, Washington University School of Medicine, St. Louis, Missouri, USA, 63110

Abstract

The delivery of luminal substances across the intestinal epithelium to the immune system is a critical event in immune surveillance resulting in tolerance to dietary antigens and immunity to pathogens. How this process is regulated is largely unknown. Recently goblet cell associated passages (GAPs) were identified as a pathway delivering luminal antigens to underlying lamina propria (LP) dendritic cells (DCs) in the steady state. Here we demonstrate that goblet cells (GCs) form GAPs in response to acetycholine (ACh) acting on muscarinic acetylcholine receptor (mAChR) 4. GAP formation in the small intestine (SI) was regulated at the level of ACh production, as GCs rapidly formed GAPs in response to ACh analogues. In contrast, colonic GAP formation was regulated at the level of GC responsiveness to ACh. Myd88 dependent microbial sensing by colonic GCs inhibited the ability of colonic GCs to respond to Ach to form GAPs and deliver luminal antigens to colonic LP-antigen presenting cells (APCs). Disruption of GC microbial sensing opened colonic GAPs and resulted in recruitment of neutrophils and APCs and production of inflammatory cytokines. Thus GC intrinsic sensing of the microbiota plays a critical role regulating the exposure of the colonic immune system to luminal substances.

Keywords

gastrointestinal tract; goblet cell; microbiota

*Correspondence should be addressed to: Rodney D. Newberry, M.D., 660 S. Euclid Avenue Box 8124, St. Louis, MO 63110, Ph: 314 362-2671, Fax: 314 362-2609, rnewberry@im.wustl.edu.

Introduction

The non-follicle bearing epithelium lining the gastrointestinal (GI) tract is the largest environmentally exposed surface in the body. This epithelium functions as a site for nutrient absorption, as a barrier separating the underlying immune system from potential pathogens, and as a site for immune surveillance of substances derived from the lumen[1,2]. How immune surveillance at the non-follicle bearing epithelium is regulated to allow education of the immune system to the luminal contents while preventing unwanted or unnecessary exposures is poorly understood.

Goblet cells (GCs) are specialized epithelial cells found in the non-follicle bearing epithelium of the GI tract. GCs have an established role in innate immunity by secreting mucins, a major component of the mucous layer, which provides a first line of defense against physical and chemical injury and protects against the invasion by pathogens[3,4]. GCs produce and secrete other biologically active products contributing to innate immunity such as trefoil peptides, resistin-like molecule β (RELMβ), and Fc-γ binding protein (Fcgbp), which respectively function to promote epithelial restitution, inhibit intestinal nematode chemotaxis, and stabilize the mucous layer[5–7]. Recently, it was discovered that when small intestine (SI) GCs secrete, they form goblet cell associated-antigen passages (GAPs) and deliver small soluble luminal antigens to lamina propria (LP) dendritic cells (DCs)[8]. GAPs were found to be the dominant mechanism for delivering luminal antigen to SI LP-DCs in the healthy steady state, as luminal antigen delivery to SI LP-DCs was undetectable when GCs and GAPs were absent[8]. Furthermore SI GAPs were dynamic, appearing and disappearing during *in vivo* imaging, and inducing GC secretion augmented GAPs and antigen delivery to SI LP-DCs, indicating that this antigen delivery mechanism may be manipulated and regulated. Notably GAPs were not seen in the colon of multiple strains of SPF housed mice despite the presence of abundant GCs and mucus indicative of GC secretion[8]. These observations suggest that there may be intrinsic differences between SI and colonic GCs, and/or that environmental differences between the SI and colon may influence the ability of GCs to form GAPs. In addition, the absence of colonic GAPs in the setting of abundant mucus could suggest that not all GC secretion is linked to GAP formation and, by extension, linked with antigen delivery. This suggests that GCs could secrete mucus to maintain the barrier and not expose the immune system to luminal contents when conditions are unfavorable for antigen delivery.

Using the above observations as a background, we investigated how GAP formation and antigen delivery to the LP immune system is regulated, including the stimuli for inducing GCs to form GAPs in the basal state. Here we demonstrate that GAP formation is driven by acetylcholine (ACh) acting on the muscarinic acetylcholine receptor (mAChR) 4. Colonic GC sensitivity to $mAChR_4$ signals, GAP formation, and luminal antigen delivery was rapidly suppressed by GC intrinsic sensing of the luminal microbiota, demonstrating a rapid and local control of antigen delivery in response to the luminal environment. Overriding GC microbial sensing to open colonic GAPs resulted in the influx of leukocytes and the production of inflammatory cytokines in the setting of the normal, non-pathogenic, microbiota. These findings identify a central role for GCs controlling the exposure of the

immune system to luminal antigens and guiding immune surveillance at the non-follicle bearing epithelium.

Results

GAP formation is driven by mAChR4 signaling in the SI in the basal state and in the colon following treatment with antibiotics

GAP formation was observed to be linked with GC secretion induced by the pan-mAChR, pannicotinic ACh receptor agonist carbamylcholine (CCh)[8]. Employing the *in vivo* imaging approach used to identify GAPs[8], we evaluated the stimuli inducing GAPs in the SI in the basal state. Following luminal administration of fluorescent 10kD dextran, GAPs were readily observed in the SI of specific pathogen free (SPF) housed C57BL/6 mice and were significantly augmented following treatment with CCh (Figure 1a,b). GAPs were not augmented by luminal (Figure 1b) or systemic (not shown) administration of cholera toxin (CT), a well studied GC secretagogue[9], demonstrating GAP formation is not linked with stimulation by all GC secretagogues. SI GAPs were effectively inhibited by atropine (Atr), a pan-mAChR antagonist (Figure 1a,b). Cholingeric agonists are known to induce GC secretion by acting directly upon GCs[10], suggesting that GAP formation could be driven by ACh acting directly on mAChRs expressed by GCs. Five mAChR subtypes, $mAChR_{1-5}$, are expressed in mammals[11]. Gene expression microarrays performed on flow cytometrically sorted GCs from the SI and colon revealed that intestinal GCs express $mAChR_3$ and $mAChR_4$ (Supplementary Figure 1), which was confirmed by using quantitative real time PCR (Figure 1c). Selective pharmacologic blockade of $mAChR_4$ by administration of tropicamide (Trop; Figure 1a,b) or himbacine (not shown), but not blockade of $mAChR_3$ by piperidine (Pip; Figure 1a,b) or 4-DAMP (not shown), effectively inhibited GAP formation in the SI, demonstrating that in the basal state ACh signaling via $mAChR_4$ drives GAP formation in the SI.

GAPs were found in the SI, but not in the colon, of multiple conventionally housed mouse strains[8]. The abundance of the microbiota is a major difference in the luminal environment between the SI and colon, with the SI harboring $\sim 10^3$ bacteria and the colon harboring $\sim 10^{11}$ bacteria per gram of intestinal contents [12]. The microbiota contributes to multiple processes including epithelial growth, metabolism, and immune stimulation[12], any of which could play a role in modulating GC secretion and GAP formation. To evaluate a role for the microbiota in GAP regulation, we treated mice with oral antibiotics to disrupt the enteric flora. We observed that SI GAPs were unchanged, but trans-epithelial columns of dextran became apparent in the colon (Figure 1d). The columns of dextran appeared on the surface epithelium and throughout the colonic crypts, were approximately the size of an epithelial cell, and contained a DAPI+ nuclei (Supplementary Movie S1). These columns were absent in the colon of antibiotic treated mice in which mouse atonal homologue 1 (Math1), a transcription factor required for GC development[13], was inducibly deleted in epithelial cells resulting in the depletion of GCs, or Math1$^{i\ vil}$ mice (Figure 1e). In the steady state the colonic epithelium does not contain Paneth cells, and within the colonic epithelium Math1 is almost exclusively expressed by GCs[14]. These columns co-localized with colonic epithelial cells with GC morphology expressing red fluorescent protein in dtom^{iMath1} reporter mice,

which labels Math1 expressing cells with the tdTomato red fluorescent protein following injection with RU486 (Figure 1f). Therefore disruption of the enteric microbiota by antibiotics allowed colonic GCs to acquire luminal fluorescent model antigen and form GAPs.

Unlike the SI, colonic GCs in conventionally housed mice were relatively unresponsive to cholinergic agonists and did not form GAPs at doses of CCh that could be given *in vivo* (Figure 1 g and i). However similar to SI GCs from conventionally housed mice, colonic GCs from antibiotic treated mice formed GAPs in the basal state, and were sensitive to exogenous cholinergic agonists *in vivo* to induce further GAP formation (Figure 1h and i). Furthermore colonic GAPs in antibiotic treated mice were inhibited by $mAChR_4$, but not $mAChR_3$, blockade (Figure 1h and i), indicating that similar pathways were inducing GAPs in the SI in the basal state and in the colon following antibiotic treatment, and suggesting that antibiotic treatment relieved the suppression of colonic GC responsiveness to $mAChR_4$ signals.

GC intrinsic Myd88 dependent microbial sensing inhibits GAP formation in the colon

To assess whether host sensing of the luminal microbiota, as opposed to other properties of the microbiota or other properties of antibiotic treatment, was regulating the ability of GCs to respond to ACh and form GAPs, we evaluated the colon of germ free (GF) mice, which lack a luminal microbiota without antibiotic treatment, and $Myd88^{-/-}$ mice, which have impaired responses to microbe-associated molecular pattern motifs via the toll-like receptors (TLRs). We observed that like the colon of antibiotic treated mice, colonic GAPs formed in GF mice and $Myd88^{-/-}$ mice, and that the colonic GAPs in these mice were inhibited by $mAChR_4$ antagonists (Figure 2a). While colonic GCs were slightly increased in GF and Myd88−/− mice, this increase is insufficient to explain the dramatic appearance of colonic GAPs in these mice, in addition GCs were not increased in antibiotic treated mice, which had a similar dramatic increase in GAPs (Supplementary Figure 2a). Similar to the SI of SPF housed mice, exogenous cholinergic agonist induced an increase in colonic GAPs in GF and SPF housed $Myd88^{-/-}$ mice, indicating that colonic GCs in mice with a reduced microbial load or altered microbial sensing became responsive to ACh via $mAChR_4$ (Figure 2b). Muscarinic AChR expression was unchanged in Myd88−/− and antibiotic treated mice (Supplementary Figure 1d), and consistent with this unresponsiveness being mediated by a rapid blockade of the $mAChR_4$ signaling pathway due to microbial sensing, we observed that heat killed cecal contents isolated from SPF housed mice inhibited colonic GAP formation within minutes upon intraluminal administration in GF mice, but not in $Myd88^{-/-}$ mice (Figure 2c). Real time PCR analysis of the cecal contents revealed no significant differences in the amount of bacteria present or changes in the ratios of the major phyla between SPF housed WT mice and $Myd88^{-/-}$ mice (Supplementary Figure 2 b and c), suggesting the alteration in microbial sensing in $Myd88^{-/-}$ mice, not differences in the microbiota account for the formation of colonic GAPs. Gene expression microarrays (Supplementary Figure 1c) and quantitative real time PCR (Figure 2d) performed on RNA isolated from GCs revealed that GCs express toll like receptors (TLRs) 1–5 and Myd88, with colonic GCs expressing much higher levels of TLRs 1, 2, 4, and 5, and SI GCs expressing slightly higher levels of TLR3. Consistent with GC intrinsic microbial sensing

regulating GAP formation, acute exposure to ligands for TLRs expressed by GCs inhibited colonic GAP formation in GF mice (Supplementary Figure 2d and e). We also observed that heat killed cecal contents or LPS could rapidly inhibit secretion in response to cholinergic stimuli in the LS174T GC line (Supplementary Figure 3a), implicating that GC intrinsic microbial sensing was able to acutely inhibit mAChR responses. To explore the role of GC intrinsic microbial sensing in regulating colonic GAP formation *in vivo*, we generated mice with an inducible deletion of Myd88 in Math1 expressing cells, which is largely restricted to GCs in the colon, or Myd88[i Math1] mice. Upon treatment with RU846, to delete Myd88 in GCs, these mice spontaneously formed GAPs in the colon (Figure 2e). Furthermore, colonic GAPs in Myd88[i Math1] mice could be augmented by treatment with CCh, a cholinergic agonist, and inhibited by $mAChR_4$ antagonists (Figure 2a,b), but were not inhibited by treatment with cecal contents (Figure 2c), consistent with GC intrinsic Myd88 dependent sensing inhibiting GCs ability to respond to $mAChR_4$ signals. Heat killed cecal contents (CC) from SPF housed mice did not inhibit SI GAP formation (Figure 2c), and consistent with this we did not see an increase in SI GAPs in Myd88[i Math1] mice (Supplementary Figure 4), indicating that GC intrinsic sensing of the microbiota plays a less prominent role in inhibiting SI GAPs in the steady state.

GC intrinsic microbial sensing activates the epidermal growth factor receptor (EGFR), p42/p44 mitogen activated protein kinase (MAPK), and suppresses mAChR₄ dependent GAP formation

In epithelial cells, ligation of TLRs, the pattern recognition receptors upstream of Myd88, can activate the epidermal growth factor receptor (EGFR)[15] and p42/p44 mitogen activated protein kinase (MAPK)[16]. In lacrimal gland GCs, p42/p44 MAPK activation represses mAChR induced secretion[17–19], suggesting that p42/p44 MAPK activation, through the EGFR, is a potential link between Myd88 dependent microbial sensing and inhibition of mAChR induced GAP formation. We observed that GCs express mRNAs for the epithelial growth factor receptor (EGFR) (Figure 2d and Supplementary Figure 1c), and consistent with this pathway blocking secretion and GAP formation, EGF activated the EGFR and p42/p44 MAPK and inhibited cholinergic agonist induced secretion in a cell intrinsic manner in the LS174T GC line (Supplementary Figure 3). Furthermore microbial products suppressed mucus secretion in a cell intrinsic manner, and this correlated with increased levels of phosphorylated EGFR and p42/p44 MAPK in the LS174T GC line (Supplementary Figure 3).

Activation of the EGFR and p42/p44 MAPK was increased *in vivo* in colonic GCs and colonic epithelium of mice with an intact microbiota and intact microbial sensing (Figure 3a and b). Further supporting GC intrinsic microbial sensing activating the EGFR and p42/p44 MAPK, deletion of Myd88 in GCs resulted in decreased activation of EGFR and p42/p44 MAPK in GCs *in vivo* in conventionally housed mice (Figure 3c). Inhibition of EGFR activation (EGFRi) or p42/p44 MAPK activation (MAPKi) reversed the suppression of GC responses to ACh imposed by host microbial sensing, and resulted in the formation of colonic GAPs in an $mAChR_4$ dependent manner in conventionally housed mice (Figure 3d and Supplementary Movie 2). Furthermore, EGF could supplant the signals delivered by microbial sensing and rapidly inhibit colonic GAPs *in vivo* in antibiotic treated mice, GF

mice, MyD88$^{-/-}$ mice, and Myd88^{i} ^{Math1} mice (Figure 3e). While cecal contents did not inhibit GAP formation in the SI, luminal EGF could inhibit SI GAPs in SPF housed mice (Figure 3f), demonstrating that the pathway downstream of the EGFR regulating GAP mAChR responsiveness and GAP formation in SI GCs was preserved. In the GF mouse colon, luminal LPS resulted in increased phosphorylation of p42/p44 MAPK and the EGFR, and inhibited GAP formation within minutes (Figure 3g and h). Colonic GAP inhibition in response to LPS was dependent upon EGFR phosphorylation (Figure 3h), demonstrating a requirement for EGFR activation downstream of microbial sensing in GAP inhibition *in vivo*. Additionally, EGF inhibition of colonic GAP formation in Abx mice, and SI GAP formation in SPF housed mice required phosphorylation of p42/p44 MAPK (Figure 3f and i), indicating that the p42/p44 MAPK activation required to suppress GAP formation is downstream of EGFR activation. Together these observations identify a pathway within colonic GCs where Myd88 signaling activates EGFR, which in turn activates p42/p44 MAPK and inhibits GC responsiveness to mAChR$_4$ signals and GAP formation.

Antigen Presenting Cells (APCs) are recruited to the colonic epithelium and acquire luminal antigen in a mAChR$_4$ dependent manner when GAPs are present

Studies using reporter mice expressing yellow fluorescent protein (YFP) driven by the CD11c promoter, or CD11c^{YFP} reporter mice [20], revealed that SI GAPs deliver luminal antigens to the CD11c^{YFP+} LP-DCs associating with the SI epithelium[8]. In contrast to the situation in the SI, we observed very few CD11c^{YFP+} cells residing near the colonic epithelium in SPF housed mice (Figure 4a–c). Most of the colonic CD11c^{YFP+} cells were deep in the LP, 30 μm below the surface. However, in SPF housed CD11c^{YFP} mice treated 24 hours prior to imaging with an inhibitor of p42/p44 MAPK (MAPKi) or EGFR (EGFRi) to induce colonic GAPs, a large number of CD11c^{YFP+} cells were found immediately below the epithelium (Figure 4a–c). Using flow cytometry to evaluate changes in the LP-DC populations after inducing colonic GAP formation with MAPK$_i$ or EGFR$_i$ revealed an influx of CD11c+MHCII+ cells, CD8^{+} T cells, and CD4^{+} T cells in both the LP and the epithelial fractions of the colon, but not the SI, where GAPs did not increase in response to MAPKi or EGFRi (Figure 4d and e, and Supplementary Figure 4 and 5). Following EGFRi treatment increases were seen in the CD103^{+} CD11b^{+} CX$_3$CR1^{-}, CD103^{-} CD11b+ CX$_3$CR1^{int}, and CD103+ CD11b+ CX3CR1^{hi} APC subsets, with the largest increase seen in the CD103+ CD11b+ CX3CR1^{hi} APC subset (Supplementary Figure 5a and b).

To evaluate if luminal antigen was effectively delivered to colonic LP antigen presenting cells (APCs) when GAPs were present, chicken egg ovalbumin (Ova) was injected into the colonic lumen, and two hours later CD103^{+} CD11c^{+} MHCII^{+} and CD103^{-} CD11c^{+} MHCII^{+} APCs were isolated from the colonic LP, excluding the colonic patches, and cultured with Ova specific CD8^{+} T cells isolated from OTI T cell receptor transgenic mice. APCs isolated from the colon of vehicle treated SPF housed mice given luminal Ova induced no increase in T cell proliferation when compared with those isolated from mice given luminal PBS (Figure 4f), indicating antigen is not effectively delivered across the colonic epithelium to LP-APCs in the basal state where GAPs are absent. In contrast, colonic LP-APCs isolated from mice given luminal Ova after treatment with an EGFRi or MAPKi to induce colonic GAPs stimulated significant OTI T cell proliferation (Figure 4f), demonstrating that luminal

antigen was effectively delivered to LP-APCs when GAPs were present. While luminal antigen was delivered to both CD103$^+$ and CD103$^-$ LP-APCs, luminal antigen was more effectively delivered to colonic CD103$^+$ LP-APCs (Figure 4f), similar to what has been reported for antigen delivery by GAPs in the SI[8]. Consistent with a requirement for GCs in this process, antigen delivery to colonic LP-APCs was not detectable when EGFRi was given to Math1$^{i\ vil}$ mice treated with RU486 to deplete GCs (Figure 4f). Furthermore, mAChR$_4$ antagonists inhibited luminal Ova delivery to colonic LP-APCs in mice given EGFRi to open colonic GAPs, but did not affect the ability of colonic LP-APCs to stimulate T cells when exogenous Ova was added to the cell culture, indicating that mAChR$_4$ antagonists inhibited delivery of antigen to LP-APCs and GAP formation, but did not affect antigen presentation capacity of LP-APCs (Figure 4g).

Overriding GC intrinsic microbial sensing and inappropriately opening colonic GAPs results in the recruitment of APCs and neutrophils and the production of inflammatory cytokines

The suppression of colonic GAPs by microbial sensing in the healthy basal state suggests that exposure of the LP immune system to substances from the colonic lumen is normally avoided, and that exposure to colonic luminal contents may have untoward outcomes despite the absence of overt pathogens in the commensal microbiota. To evaluate the effect of prolonged opening of colonic GAPs in the setting of the normal commensal flora and intact microbial sensing by the immune system, we treated Myd88$^{i\ Math1}$ mice or their littermates, Myd88$^{fl/fl}$ mice, with sequential injections of RU486 over the course of four days and evaluated the LP-DC populations and antigen delivery in the colon. Similar to mice treated with EGFRi or MAPKi, changes in the LP-APC populations were also observed in Myd88$^{i\ Math1}$ mice lacking Myd88 specifically in GCs (Figure 5a and b). However, there was not an increase in colonic LP-APCs in mice lacking Myd88 globally (Figure 5b) or in EGFRi or MAPKi treated mice given antibiotics (Figure 5c), implicating a role for Myd88 dependent microbial sensing in cell types other than GCs in recruiting cellular populations in the colon when GAPs were present. Confirming antigen delivery occurs in the colon of mice lacking Myd88 in GC, colonic APCs isolated from Myd88$^{i\ Math1}$ mice, and not those isolated from Myd88$^{fl/fl}$ littermate mice, given RU486 and luminal Ova, induced T cell proliferation in *ex vivo* assays (Figure 5d).

Myd88$^{i\ Math1}$ mice with colonic GAPs opened for four days had significantly elevated production of IL-6 in the MLN and colonic LP and significantly elevated IL-17 in the colonic LP with a trend toward elevated production of IL-6 in the serum (Figure 5e). We also observed elevated production of the neutrophil chemoattractant CXCL1 and an influx of neutrophils in the colonic mucosa (Figure 5f–i) indicative of an acute inflammatory response. Therefore inhibiting GC intrinsic microbial sensing and inappropriately delivering luminal contents to the normal colonic immune system resulted in an inflammatory response in the absence of an overt pathogenic infection.

Discussion

The primary function of the non-follicle bearing epithelium of the GI tract is absorption of nutrients, requiring that this be a single layer expansive epithelial surface that is exposed to the environment. In addition to absorption, the epithelium also forms a barrier protecting the host from potential pathogens. Furthermore, combining observations from multiple studies implicates the non-follicle bearing epithelium as a site of immune surveillance, which is important for homeostatic responses to innocuous antigens, such as tolerance to dietary antigens, and for immunity to pathogens[2,21–23]. How the epithelium and the underlying immune system within the LP simultaneously perform these diverse functions of barrier maintenance, absorption, and immune surveillance has been a question of significant interest in mucosal immunology.

While multiple pathways delivering macromolecular substances from the lumen across the intestinal epithelium have been identified, the relative importance of each pathway in LP immune surveillance different settings and how each pathway is regulated to control access to luminal substances to the immune system are largely uninvestigated. The epithelial layer of the GI tract maintains its protective barrier in part through the formation of tight junctions between epithelial cells, which can allow luminal substances to cross the epithelium via a pore formed by claudin proteins that allows small solutes to pass[24], and via paracellular leak pathway that allows larger macromolecules including proteins and carbohydrates to cross the epithelial barrier[25]. Paracellular leak was reported to be present in mice lacking GCs, but luminal antigen was not effectively delivered to SI LP-DCs as assessed by their inability to induce antigen specific T cell responses[8], suggesting that paracellular leak may not effectively deliver antigen to LP-DCs in the steady state. Alterations in tight junctions and paracellular leak resulting in increased flux across the epithelium have been associated with a predisposition to develop inflammation and overt inflammation[25,26], suggesting that this pathway could be an important contributor to disease processes. Therefore, while the immune outcomes downstream of antigen delivery via paracellular leak are not well understood, observations suggest this pathway may not play a major role in steady state immune surveillance.

Microfold (M) cell-mediated transcytosis is the most studied mechanism delivering antigen across the intestinal epithelium to the immune system. The vast majority of M cells are found as part of the follicle associated epithelium overlying lymphoid follicles, with rare M cells located in the villous epithelium in the SI steady state[27,28]. Current understanding is that M cells continuously deliver antigens to the underlying immune system irrespective of the types of antigen and environmental stimuli, suggesting that regulation of antigen delivery to the LP via M cells would require altering the number of villous M cells. Villous M cell numbers can increase in number in response to environmental stimuli including exogenous toxins and endogenous cytokines[28,29] however this requires days, indicating that regulating antigen delivery via M cells in this manner is not rapid. Moreover, the rarity of villous M cells in the SI and their apparent absence in the non-follicle bearing epithelium in the colon, suggests that villous M cells would be minor contributors to steady state LP immune surveillance.

Multiple studies have described the ability of LP-DCs to pass dendrites between epithelial cells and extend them into the lumen to acquire luminal substances and bacteria[30–34]. When observed, LP-DC trans-epithelial dendrites (TEDs) have largely been noted in the SI as opposed to the colon. Similar to our findings here regarding GC mediated antigen delivery, epithelial Myd88 dependent sensing of the microbiota regulated TED formation by LP-DCs[32], and accordingly would regulate luminal antigen access to the LP immune system. However, in contrast to our findings of antigen delivery by colonic GCs, TED formation by LP-DCs was induced[32], not inhibited by the microbiota. These observations demonstrate reciprocal regulation of antigen access to the LP immune system by GCs and LP-DC TED formation and imply different contributions of these antigen delivery mechanisms. The microbial stimuli regulating antigen delivery need not be pathogenic, as the commensal microbiota can inhibit colonic GAPs and LP-DC TED formation has been observed in the absence of enteric infection[31,32].

Recently it was discovered that when GCs secrete they can form GAPs and deliver luminal antigens to LP-DCs in the SI[8], suggesting that this could be a mechanism whereby the epithelium allows immune surveillance of the luminal contents, while simultaneously maintaining the barrier with mucus secretion. The ability to augment GAPs and antigen delivery by agents inducing GC mucous secretion, the dynamic nature of GAPs, appearing and disappearing during the imaging window, and the lack of GAPs in the colon despite the presence of abundant GCs[8], suggested that GAP formation and antigen delivery could be regulated. In addition, Mucin 2, a goblet cell-derived component of mucus, was found to imprint DCs with tolerogenic signals [35] suggesting that when GCs secrete they can form GAPs to deliver luminal antigens in the context of tolerogenic signals to DCs. Here we identify that in the basal state SI GAP formation is driven by ACh acting on the $mAChR_4$. Notably, CT, a well-known GC secretagogue, did not induce GAP formation, demonstrating that not all stimuli inducing GC secretion induce GAPs. GCs are known to secrete by two pathways, compound exocytosis, an intracellular Ca^{2+} driven pathway in which multiple vesicles of mucin fuse and are secreted, and primary exocytosis, a cAMP driven pathway in which single mucin vesicles fuse with the plasma membrane during secretion[9,36–38]. The association of GAP formation with ACh induced secretion, which occurs by compound exocytosis, but not with cholera toxin induced secretion, which occurs by primary exocytosis, suggests that GAP formation could be linked with specific types of GC secretion. This may allow GCs to secrete mucus to maintain the barrier and not form GAPs to deliver luminal antigens in situations where antigen delivery to the immune system could be unfavorable.

Colonic GCs were unresponsive to ACh to form GAPs and deliver antigen to the colonic LP-APCs when the luminal microbiota and GC intrinsic microbial sensing were intact. Disruption of either the microbiota or of GC microbial sensing relieved the repression of the $mAChR_4$ pathway in colonic GCs and induced GAPs to form, which allowed luminal antigen delivery to both CD103^{+} and CD103^{−} colonic LP-APCs, with more effective delivery to CD103+ colonic LP-APCs. This could suggest that both LP-APC populations interact with the colonic GAPs with the CD103+ LP-APCs interacting with GAPs more frequently.

—

Recently Mazzini et al reported a critical role for gap junction dependent antigen transfer between SI LP-DCs in the acquisition of luminal antigen[39]. Similar to the report describing SI GAPs[8], Mazzini et al found that luminal antigen was only effectively delivered to CD103+ LP-DCs as assessed by the ability to induce antigen specific T cell responses[39]. Moreover antigen delivery to CD103+ LP-DCs was found to be dependent upon the DC expression of the gap junction protein connexin 43 in one study and and upon GCs in the other, as deletion of either connexin 43 in DCs or deletion of GCs, via deletion of Math1 in intestinal epithelial cells, abolished luminal antigen delivery to SI CD103+ LP-DCs[8,39]. Of note, gap junction proteins, including connexin 43, are expressed by GCs, as determined by gene expression microarrays. These observations raise the possibility that these pathways may be related.

Shutting down colonic GAPs by microbial ligands or opening up colonic GAPs by manipulating microbial sensing or the downstream EGFR p42/p44 MAPK pathway occurred rapidly. Heat-killed cecal contents and TLR ligands were sufficient to inhibit GAP formation, indicating that live bacteria are not required for this process and suggesting GCs may sense microbial products which can gain access to the epithelium through the mucus layer, which acts as a physical barrier preventing whole bacteria from contacting the epithelium in the colon[40]. In combination with the GC intrinsic nature of these events, these observations indicate that regulation of antigen delivery by GAPs is rapid and local, and that colonic GCs are active participants in immune surveillance by controlling the immune system's access to luminal antigens.

Interestingly we observed that SI GAPs were not rapidly shut down in response to heat killed cecal contents and they were unchanged in mice lacking Myd88 in GCs, indicating that SI GCs were relatively unresponsive to microbial ligands. SI GCs expressed lower levels of TLRs and higher levels of inhibitors of TLR signaling, as seen by gene expression microarrays, which could explain their relative unresponsiveness to microbial ligands and suggests that GC sensing of microbial stimuli does not play a major role suppressing SI GAPs in the normal steady state. While the SI expresses similar levels of EGFR, phosphorylated EGFR could not be detected, demonstrating that unlike the colon, EGFR activation in SI GCs is absent at the steady-state. However, SI GAPs could still be shut off with exogenous EGF, through activation of p42/p44 MAPK, indicating that similar regulatory pathways of mAChR$_4$ responsiveness are present in SI GCs. The significance of retaining the pathways downstream of the EGFR that inhibit mAChR$_4$ responses in SI GCs in the setting of the relative inability of microbial ligands to shut off SI GAPs, is unclear, but could suggest that in some situations, such as enteric infection, SI GCs may alter their responsiveness to microbial stimuli, potentially via increased TLR expression or decreased expression of inhibitors of TLR signaling, and shut off GAPs similar to colonic GCs. A further implication of these observations is that in the steady state, luminal antigen delivery to the SI LP-APCs is largely regulated by ACh production and release, which is predominantly neuronal in origin, suggesting situations in which the presence or absence of antigen delivery to the SI LP could be linked to environmental stimuli inducing neuronal production of ACh.

The absence of GAPs and antigen delivery to LP-APCs, combined with the spatial separation of LP-APCs from the colonic epithelium we observed *in vivo* in healthy wildtype SPF housed mice, suggests that in the steady state the colonic LP immune system is relatively unaware of the colonic luminal contents. Immune surveillance in this situation may primarily occur through the follicle-associated epithelium overlying the colonic patches and lymphoid follicles. GCs have been reported in the follicle associated epithelium (FAE)[41] and rare GAPs have been noted on the periphery of the FAE overlying the cecal path in the steady state[8], how these are regulated and if these contribute to immune surveillance remains to be explored. Intrinsic differences in the function of the SI and colon could justify the difference in antigen delivery and interactions of APCs with the epithelium between the two organs, with the SI actively absorbing dietary nutrients, which the immune system may survey to induce tolerance, and the colon largely absorbing water and solutes, which are not readily recognized by the adaptive immune system. This difference could also be attributed to the more abundant and complex microbial stimuli in the colon, which makes recognizing and appropriately responding to innocuous antigens in this environment tenuous. In support of the latter possibility we observed that opening colonic GAPs for four days resulted in the production of inflammatory cytokines and chemokines and an influx of leukocytes including neutrophils, indicative of acute inflammation, despite the lack of overt pathogens in the commensal microbiota. This suggests that the lack of antigen delivery to the colonic LP immune compartment is not primarily to promote ignorance or disinterest, but to avoid inappropriate responses by the colonic LP immune system to luminal antigens encountered in a complex microbial environment.

The intestinal epithelium performs the diverse and essential functions of absorption, barrier maintenance, and immune surveillance. How the immune system gains access to luminal antigens without compromising the epithelial barrier and absorption, and how the immune system appropriately responds to innocuous antigens encountered in a complex environment of abundant microbiota and microbial stimuli are central questions in intestinal immunology. Here we identify the stimuli and pathways regulating GAP formation and luminal antigen delivery to LP-APCs in the steady state and further link this process with GC secretion. These observations demonstrate novel ways in which GCs contribute to diverse epithelial functions and uncover a central role for colonic GC sensing of the luminal microbiota to regulate the immune system's exposure and access to luminal substances.

Methods

Mice

All mice used in these studies were on the C57BL/6 background. C57BL/6 mice were purchased from The National Cancer Institute (Frederick, MD) or The Jackson Laboratory (Bar Harbor, MN). OTI T cell receptor transgenic mice[42], Math1^{fl/fl} mice[13], Math1[PGRCre] mice[43], CD11c[YFP] transgenic mice[20], CX$_3$CR1[GFP] mice[44], and ROSA[dtomato] mice[45], mice were purchased from The Jackson Laboratory. Myd88^{−/−} mice[46], a gift from Dr. Akira (Osaka University, Osaka, Japan), were bred onto the C57BL/6 background by the Speed Congenics Facility of the Rheumatic Diseases Core Center, and maintained in house. Transgenic mice bearing a tamoxifen-dependent Cre recombinase expressed under the

control of the villin promoter (vil-Cre-ERT2) mice [47] were a gift from Sylvie Robine (Institut Curie, Paris, France). Math1$^{fl/fl}$ mice were bred to vil-Cre-ERT2 mice to generate mice with inducible depletion of GCs following deletion of Math1 in villin expressing cells, referred to as Math1$^{i\ vil}$ mice. To deplete GCs, Math1$^{i\ vil}$ mice mice were injected with 100 µg tamoxifen (Sigma-Aldrich, St. Louis, MO, USA) dissolved in sunflower seed oil with 20% ethanol (Sigma-Aldrich) i.p. daily for 4 days. Three days after the final injection, mice were placed on antibiotics for one week and then analyzed for GAP formation by two-photon as described below. Colon tissue was sectioned and stained for goblet cells with alcian blue to ensure goblet cells were knocked out. To generate Math1 reporter mice, Math1^{PGRCre} mice, which express a progesterone inducible Cre under the control of the Math1 locus, were bred with ROSA^{dtomato} mice, referred to as dtom^{iMath1} mice. To label colonic GCs, dtom^{iMath1} mice were injected with 200 µg RU486 (mifepristone, Caymen Chemicals, Ann Arbor, MI, USA) dissolved in sesame oil (Acros Organics, Sigma-Aldrich) i.p. every day for 7 days. To delete Myd88 signaling from GCs, Myd88$^{fl/fl}$ mice were bred to Math1^{PGRcre} mice, referred to as to Myd88$^{i\ Math1}$ mice. To induce deletion of Myd88 in GCs, Myd88$^{i\ Math1}$ mice were injected with 200 µg RU486 i.p. on day 0 and day 2, and analyzed on day 4. Myd88$^{fl/fl}$ Math1^{WT} littermate mice injected with RU486 were used for controls. Gnotobiotic mice were obtained from the Washington University Digestive Disease Research Core Center murine models core. Animals, other than gnotobiotic mice, were housed in a specific-pathogen-free facility and fed routine chow diet. In some experiments mice were treated with a combination of antibiotics (Abx); ampicillin (1 g/L), metronidazole (1 g/L), neomycin (1 g/L), and vancomycin (500 mg/L) in drinking water for 10 days. Animals were 6 to 16 weeks of age at the time of analysis. Animal procedures and protocols were carried out in accordance with the institutional review board at Washington University School of Medicine.

Isolation of cellular populations and flow cytometric sorting

Small intestines were harvested, rinsed with PBS and Peyer's Patches were removed. Epithelium associated DCs and T cells were released by incubating for 15 min two times in a 37°C rotating incubator in HBSS media (BioWhittaker, Walkersville, Maryland) containing 5 mM EDTA as previously described[48]. After a third incubation with HBSS media with 5 mM EDTA, isolation of splenic and lamina propria (LP) cellular populations was performed as previously described[48]. Cellular suspensions were then passed through a 50µm nylon filter and the cells were prepared for flow cytometric analysis or sorting. Antibodies used for analysis are listed in supplemental table I. DC subpopulations in the SI or APCs in the colon were identified as 7AAD$^-$, CD45$^+$, CD11c$^+$, MHCII$^+$ and either CD103$^+$ or CD103$^-$ for flow cytometric sorting. To isolate goblet cells, small intestinal or colonic epithelium was released by incubating for 15 minutes in 37 °C rotating incubator in HBSS media (BioWhittaker, Walkersville, Maryland) containing 5 mM EDTA as previously described. Goblet cells were identified as CD45$^-$CD24$^-$CK-18$^+$UEA-1$^+$, while IECs were identified as CD45$^-$CD24$^-$CK-18$^-$UEA-1$^-$, and sorted directly into RLT buffer (Qiagen, Valencia, CA, USA) for RNA extraction.

Immunohistochemistry

Immunohistochemistry on frozen sections was performed as previously described[48]. Antibodies used for immunohistochemistry are listed in supplemental table I. Pseudo-colored black and white images from fluorescent microscopy were obtained with an axioskop 2 microscope using Axiovision software (Carl Zeiss MicroImaging, Thornwood, NY).

Intravital two-photon (2P) microscopy

Mice were anesthetized using nebulized isofluorane in 95% O_2/5% CO_2. Intravital preparation of the small intestine was performed as previously described[8]. Briefly a small midline vertical incision was made through the skin and peritoneum revealing the intestine. To image from the luminal surface, a 7 mm incision was made to expose the luminal surface of the small intestine. Large fecal particles were removed with care to prevent damaging the luminal surface. Smaller fecal particles were more difficult to remove and in order to avoid disrupting the mucous layer and the epithelia, were left in place. Imaging was performed with the intestine remaining within the peritoneal cavity. Fluorescently labeled dextran 10,000 MW (10 mg/mL, Invitrogen, Carlsbad, CA, USA) and diamidino-2-phenylindole (DAPI; 10 mg/mL, Invitrogen) were injected intraluminally as described previously[8] to identify GAPs. Tissues were excited using a Ti:sapphire laser tuned to 890nm (Chameleon XR, Coherent). In some experiments mice were given the following treatments before intraluminal dextran administration: 600mg/kg atropine chloride (Sigma-Aldrich) i.p 2 hours prior, 150mg/kg carbamylcholine (Sigma-Aldrich) i.p 10 minutes prior, 100mg/kg tropicamide or 100mg/kg 4-DAMP, (mAChR$_4$ selective antagonists, Sigma-Aldrich) i.p. 20 minutes prior, 100mg/kg piperidine or 100mg/kg himbacine, (mAChR$_3$ selective antagonists, Sigma-Aldrich) i.p. 20 minutes prior, 500μg/kg tryphostin AG1478 (inhibitor of EGFR phosphorylation, Sigma-Aldrich) i.p. 20 minutes prior, 10μg murine recombinant EGF (Shenandoah Biotechnologies, Warwick, PA, USA) injected intraluminally 20 minutes prior, 10 μg LPS (Sigma-Aldrich) injected intraluminally 20 minutes prior, or 10mg/kg U-0126 (inhibitor of p42/p44 MAPK phosphorylation, Sigma-Aldrich) i.p. 20minutes prior. Cecal contents from a SPF-housed mouse was resuspended in 1 ml PBS and heat-killed at 95°C for 30 minutes and 50 μl of this suspension was injected intraluminally 20 minutes prior to dextran administration. After imaging, tissue was fixed with 10% formalin buffered solution for 30 minutes before OCT embedding.

Enumeration of GAPs

GAPs were identified as dextran-filled columns measuring approximately 20μm (height) × 5μm (diameter) traversing the epithelium and containing a nucleus. When present, colonic GAPs were found all regions of the colon examined, both on the surface epithelium and within the crypts. GAPs were enumerated in the jejunum or mid-transverse colon using Z-stack images of a volume of 225μm(x) by 250μm(y) by 50μm(z) acquired during a 20 minute imaging window beginning 20 minutes after dextran administration. SI GAPs were enumerated as GAPs per villus and colonic GAPs were enumerated within the crypts as GAPs per crypt, which were identified as a ring of DAPI$^+$ epithelial nuclei with fluorescent dextran in the lumen (center). The number of GAPs per villus and GAPs per crypt seen by

2P imaging were confirmed by immunofluorescence microscopy of tissues that were fixed following 2P imaging.

Ex vivo analysis of effect of TLR ligands on GAP formation

Colonic tissue from germfree housed mice were cut into 2cm pieces and placed in a 48 well culture plate containing 500 µl media containing 10% FBS, with fluorescent dextran 10,000 MW (10 mg/mL), and, in some conditions, 10 µg/ml LPS, 10 µg/ml LTA, or 10 µg/ml PolyI:C, and incubated for 30 minutes at 37 C. Tissue was fixed with 10% formalin buffered solution for 30 minutes before OCT embedding.

Cell Culture

The LS 174T cell line, a gift from Dr. Rex Gaskins (University of Illinois, Champaign, Illinois) was maintained per the recommendations of American Type Culture Collection (Manassas, VA), and plated on 6 well culture plates for assays. For secretion assays, cells were serum starved for 1 hour, then fresh media was added along with 10 µM carbamylcholine and incubated for 30 minutes at 37°C. The supernatent was centrifuged and Muc5ac was measured by ELISA. In some experiments 10 µg/ml LPS, 10 µg/ml recombinant human EGF (Shenandoah Biotechnologies), 5 µl heat-killed cecal contents, 1 µg/ml tryphostin AG1478 (EGFRi), or 10 µg /ml U-0126 (MAPKi), were added for 30 minutes prior to carbamycholine addition, during serum starvation.

ELISAs

Muc5ac secreted by LS174T cells was measured by an ELISA comprised of a polyclonal Muc5AC antibody (#Ab78660, Abcam, Cambridge, UK) for capture, and biotin-labeled monoclonal (#MS-145-B, Thermo Fisher Scientific, Runcorn, UK) for detection, and compared to a standard curve with recombinant protein (#H00004586-Q01 Novus Biologicals, Littleton, CO, USA). Phosphorylated p42/p44 MAPK (R&D Systems, Minneapolis, MN, USA), phosphorylated EGFR (R&D Systems), IL-6 (R&D Systems), IL-17 (R&D Systems), and CXCL1 (R&D Systems) were measured using ELISA per the manufacturers recommendations. Phosphorylated p42/p44 MAPK and phosphorylated EGFR were measured on 1/32 and 1/216, respectively, of the epithelial cell population removed from the intestine or colon by one incubation in HBSS containing 5mM EDTA at 37°C for 15 minutes. IL-6 and IL-17 was measured from the supernatant of MLN cells and LP cells isolated as described above and cultured at a density of 5×10^6/ml in RPMI media containing 10% fetal calf serum, 5×10^{-5}M 2-ME, 2mM L-glutamine, 10mM HEPES, 50U/ml penicillin, 50µg/ml streptomycin, and 1mM sodium pyruvate at 37°C 5% CO_2 for three days. CXCL1 was measured in whole intestine homogenized in sterile PBS.

Evaluation of gene expression in GCs

RNA was extracted from flow cytometrically sorted GC populations identified and isolated as described above. Gene expression microarrays were performed on four independent isolates of SI or colon GCs by the Genome Technology Access Center at Washington University School of Medicine using the Illumina Mouse 8 TotalPrep platform. Analysis of microarray data was performed using Partek Genomics Suite (St. Louis, MO). For

quantitative real time polymerase chain reaction assays, RNA was extracted from GC populations isolated as above, treated with DNAse, and transcribed into cDNA using Superscript II reverse transcriptase (Invitrogen) according to the manufacturer's recommendations. Primers used for RT-PCR described in supplemental table 2. The absolute copy number of the target was calculated from standards that were constructed as previously described [49].

Analysis of luminal antigen delivery to LP-DCs

Mice were anesthetized and 2mg of ovalbumin (Sigma-Aldrich) dissolved in phosphate buffered saline (PBS), or PBS alone (controls) was injected into the lumen of the SI or colon. Two hours after the administration of ovalbumin, cell populations were isolated from the non-follicle bearing LP as previously described[49] and sorted by flow cytometry. Sorted DC populations were cultured with flow cytometric sorted CD3+, CD8α+, Vα2+, Vβ8+ splenic T cells from OTI transgenic mice at a ratio of 1:10 DC to T cells. As a positive control, 20μg of Ova was added to cultures of DC populations isolated from mice receiving luminal PBS. After 3 days cultures were evaluated for the number of T cells by flow cytometry and cell counting.

Statistical Analysis

Data analysis using a student's *t* test was performed using GraphPad Prism (GraphPad Software Inc., San Diego, CA). Microarray analysis preformed with JMP Genomics (SAS Institute, Cary, NC). Statistical significance was defined as p<0.05.

Supplementary Material

Refer to Web version on PubMed Central for supplementary material.

Acknowledgements

References

1. Eri R, Chieppa M. Messages from the Inside. The Dynamic Environment that Favors Intestinal Homeostasis. Frontiers in immunology. 2013; 4:323. [PubMed: 24130559]

2. Peterson LW, Artis D. Intestinal epithelial cells: regulators of barrier function and immune homeostasis. Nat Rev Immunol. 2014; 14:141–153. [PubMed: 24566914]

3. Johansson ME, Hansson GC. Is the intestinal goblet cell a major immune cell? Cell host & microbe. 2014; 15:251–252. [PubMed: 24629330]

4. Kim YS, Ho SB. Intestinal goblet cells and mucins in health and disease: recent insights and progress. Curr Gastroenterol Rep. 12:319–330. [PubMed: 20703838]

5. Taupin D, Podolsky DK. Trefoil factors: initiators of mucosal healing. Nat Rev Mol Cell Biol. 2003; 4:721–732. [PubMed: 14506475]

6. Herbert DR, et al. Intestinal epithelial cell secretion of RELM- protects against gastrointestinal worm infection. Journal of Experimental Medicine. 2009; 206:2947–2957. [PubMed: 19995957]

7. Johansson ME, Thomsson KA, Hansson GC. Proteomic analyses of the two mucus layers of the colon barrier reveal that their main component, the Muc2 mucin, is strongly bound the Fcgbp protein. J Proteome Res. 2009; 8:3549–3557. [PubMed: 19432394]

8. McDole JR, et al. Goblet cells deliver luminal antigen to CD103+ dendritic cells in the small intestine. Nature. 2012; 483:345–349. [PubMed: 22422267]

9. Epple HJ, et al. Differential stimulation of intestinal mucin secretion by cholera toxin and carbachol. Pflugers Arch. 1997; 433:638–647. [PubMed: 9049150]

10. Hodges RR, et al. Signaling pathways used by EGF to stimulate conjunctival goblet cell secretion. Experimental eye research. 2012; 103:99–113. [PubMed: 22975404]

11. Wess J, Eglen RM, Gautam D. Muscarinic acetylcholine receptors: mutant mice provide new insights for drug development. Nature reviews. Drug discovery. 2007; 6:721–733. [PubMed: 17762886]

12. Neish AS. Microbes in gastrointestinal health and disease. Gastroenterology. 2009; 136:65–80. [PubMed: 19026645]

13. SHROYER N, et al. Intestine-Specific Ablation of Mouse atonal homolog 1 (Math1) Reveals a Role in Cellular Homeostasis. Gastroenterology. 2007; 132:2478–2488. [PubMed: 17570220]

14. Shroyer NF, Wallis D, Venken KJ, Bellen HJ, Zoghbi HY. Gfi1 functions downstream of Math1 to control intestinal secretory cell subtype allocation and differentiation. Genes Dev. 2005; 19:2412–2417. [PubMed: 16230531]

15. Koff JL, Shao MX, Ueki IF, Nadel JA. Multiple TLRs activate EGFR via a signaling cascade to produce innate immune responses in airway epithelium. American journal of physiology. Lung cellular and molecular physiology. 2008; 294:L1068–L1075. [PubMed: 18375743]

16. Cario E, et al. Lipopolysaccharide activates distinct signaling pathways in intestinal epithelial cell lines expressing Toll-like receptors. J Immunol. 2000; 164:966–972. [PubMed: 10623846]

17. Keely SJ, Calandrella SO, Barrett KE. Carbachol-stimulated transactivation of epidermal growth factor receptor and mitogen-activated protein kinase in T(84) cells is mediated by intracellular ca(2+), PYK-2, and p60(src). J Biol Chem. 2000; 275:12619–12625. [PubMed: 10777553]

18. Dartt DA. Neural regulation of lacrimal gland secretory processes: relevance in dry eye diseases. Prog Retin Eye Res. 2009; 28:155–177. [PubMed: 19376264]

19. Ota I, et al. Alpha 1-adrenergic and cholinergic agonists activate MAPK by separate mechanisms to inhibit secretion in lacrimal gland. American journal of physiology. Cell physiology. 2003; 284:C168–C178. [PubMed: 12388118]

20. Lindquist RL, et al. Visualizing dendritic cell networks in vivo. Nat Immunol. 2004; 5:1243–1250. [PubMed: 15543150]

21. Knoop KA, Miller MJ, Newberry RD. Transepithelial antigen delivery in the small intestine: different paths, different outcomes. Curr Opin Gastroenterol. 2013; 29:112–118. [PubMed: 23380572]

22. Spahn TW, Kucharzik T. Modulating the intestinal immune system: the role of lymphotoxin and GALT organs. Gut. 2004; 53:456–465. [PubMed: 14960534]

23. Worbs T, et al. Oral tolerance originates in the intestinal immune system and relies on antigen carriage by dendritic cells. J Exp Med. 2006; 203:519–527. [PubMed: 16533884]

24. Shen L, Weber CR, Raleigh DR, Yu D, Turner JR. Tight Junction Pore and Leak Pathways: A Dynamic Duo. Annual Review of Physiology. 2011; 73:283–309.

25. Turner JR. Intestinal mucosal barrier function in health and disease. Nat Rev Immunol. 2009; 9:799–809. [PubMed: 19855405]

26. Su L, et al. Targeted epithelial tight junction dysfunction causes immune activation and contributes to development of experimental colitis. Gastroenterology. 2009; 136:551–563. [PubMed: 19027740]

27. Jang MH, et al. Intestinal villous M cells: an antigen entry site in the mucosal epithelium. Proc Natl Acad Sci U S A. 2004; 101:6110–6115. [PubMed: 15071180]

28. Knoop KA, et al. RANKL Is Necessary and Sufficient to Initiate Development of Antigen-Sampling M Cells in the Intestinal Epithelium. The Journal of Immunology. 2009; 183:5738–5747. [PubMed: 19828638]

29. Terahara K, et al. Comprehensive gene expression profiling of Peyer's patch M cells, villous M-like cells, and intestinal epithelial cells. Journal of immunology (Baltimore, Md. : 1950). 2008; 180:7840–7846.

30. Rescigno M, et al. Dendritic cells express tight junction proteins and penetrate gut epithelial monolayers to sample bacteria. Nat Immunol. 2001; 2:361–367. [PubMed: 11276208]

31. Niess JH. CX3CR1-Mediated Dendritic Cell Access to the Intestinal Lumen and Bacterial Clearance. Science. 2005; 307:254–258. [PubMed: 15653504]

32. Chieppa M, Rescigno M, Huang AY, Germain RN. Dynamic imaging of dendritic cell extension into the small bowel lumen in response to epithelial cell TLR engagement. J Exp Med. 2006; 203:2841–2852. [PubMed: 17145958]

33. Vallon-Eberhard A, Landsman L, Yogev N, Verrier B, Jung S. Transepithelial pathogen uptake into the small intestinal lamina propria . Journal of immunology (Baltimore, Md. : 1950). 2006; 176:2465–2469.

34. Farache J, et al. Luminal bacteria recruit CD103+ dendritic cells into the intestinal epithelium to sample bacterial antigens for presentation. Immunity. 2013; 38:581–595. [PubMed: 23395676]

35. Shan M, et al. Mucus enhances gut homeostasis and oral tolerance by delivering immunoregulatory signals. Science. 2013; 342:447–453. [PubMed: 24072822]

36. Specian RD, Neutra MR. Mechanism of rapid mucus secretion in goblet cells stimulated by acetylcholine. J Cell Biol. 1980; 85:626–640. [PubMed: 7391135]

37. Neutra MR, O'Malley LJ, Specian RD. Regulation of intestinal goblet cell secretion. II. A survey of potential secretagogues. Am J Physiol. 1982; 242:G380–G387. [PubMed: 7065260]

38. Pickett JA, Edwardson JM. Compound exocytosis: mechanisms and functional significance. Traffic. 2006; 7:109–116. [PubMed: 16420520]

39. Mazzini E, Massimiliano L, Penna G, Rescigno M. Oral Tolerance Can Be Established via Gap Junction Transfer of Fed Antigens from CX3CR1 Macrophages to CD103 Dendritic Cells. Immunity. 2014

40. Johansson ME, Larsson JM, Hansson GC. The two mucus layers of colon are organized by the MUC2 mucin, whereas the outer layer is a legislator of host-microbial interactions. Proc Natl Acad Sci U S A. 108(Suppl 1):4659–4665. [PubMed: 20615996]

41. Ermund A, Gustafsson JK, Hansson GC, Keita AV. Mucus properties and goblet cell quantification in mouse, rat and human ileal Peyer's patches. PLoS One. 2013; 8:e83688. [PubMed: 24358305]

42. Hogquist KA, et al. T cell receptor antagonist peptides induce positive selection. Cell. 1994; 76:17–27. [PubMed: 8287475]

43. Rose MF, Ahmad KA, Thaller C, Zoghbi HY. Excitatory neurons of the proprioceptive, interoceptive, and arousal hindbrain networks share a developmental requirement for Math1. Proc Natl Acad Sci U S A. 2009; 106:22462–22467. [PubMed: 20080794]

44. Jung S, et al. Analysis of fractalkine receptor CX(3)CR1 function by targeted deletion and green fluorescent protein reporter gene insertion. Mol Cell Biol. 2000; 20:4106–4114. [PubMed: 10805752]

45. Madisen L, et al. A robust and high-throughput Cre reporting and characterization system for the whole mouse brain. Nature neuroscience. 2010; 13:133–140. [PubMed: 20023653]

46. Adachi O, et al. Targeted disruption of the MyD88 gene results in loss of IL-1- and IL-18-mediated function. Immunity. 1998; 9:143–150. [PubMed: 9697844]

47. el Marjou F, et al. Tissue-specific and inducible Cre-mediated recombination in the gut epithelium. Genesis. 2004; 39:186–193. [PubMed: 15282745]

48. McDonald KG, et al. Epithelial expression of the cytosolic retinoid chaperone cellular retinol binding protein II is essential for in vivo imprinting of local gut dendritic cells by lumenal retinoids. Am J Pathol. 2012; 180:984–997. [PubMed: 22222225]

49. McDonald KG, McDonough JS, Dieckgraefe BK, Newberry RD. Dendritic cells produce CXCL13 and participate in the development of murine small intestine lymphoid tissues. Am J Pathol. 2010; 176:2367–2377. [PubMed: 20304952]
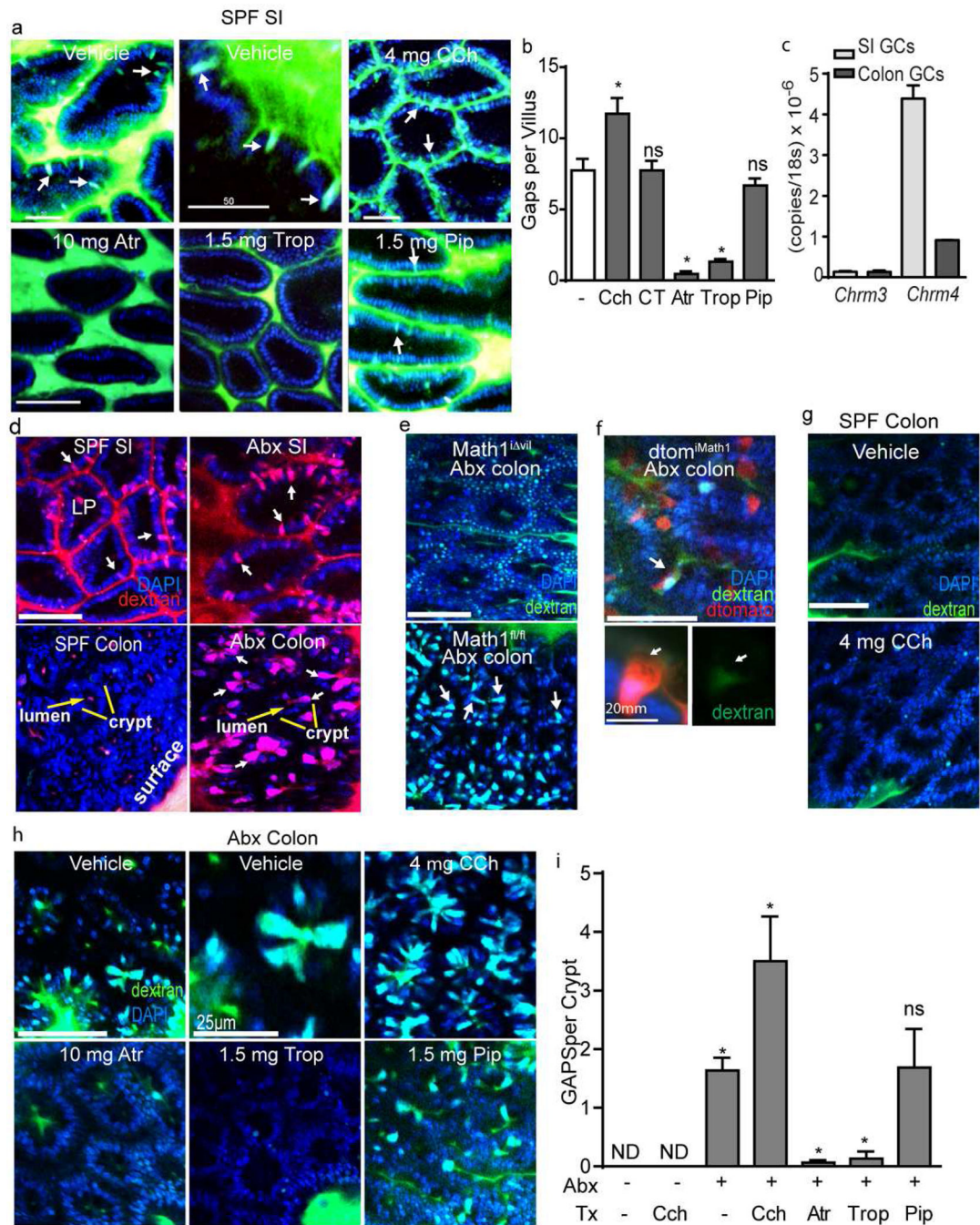
Figure 1. GAP formation is driven by mAChR₄ signaling in the SI at the basal state and in the colon following treatment with antibiotics

a) Intravital two-photon (2P) images of the SI following the luminal administration of dextran (green) and DAPI (blue) and b) number of GAPs per villus from mice treated with carbamylcholine (CCh; a pan-nicotinic pan-muscarinic receptor agonist), atropine (Atr; a pan-muscarinic receptor antagonist), tropicamide (Trop; a mAChR₄ antagonist), piperidine (Pip; a mAChR₃ antagonist), or cholera toxin (CT; a GC secretagogue, in b only). c) Quantitative real time RNA for the genes encoding mAChR₃ and mAChR₄ (*Chrm3* and

Chrm4 respectively) from FACS sorted SI and colonic goblet cells. d) 2P images of the SI and colon following the administration of luminal dextran (red) and DAPI (blue) in SPF-housed mice untreated or treated with antibiotics (Abx). e) 2P images of the colon of Math1[i vil] mice or littermate controls treated with tamoxifen and antibiotics following the administration of luminal dextran (green) and DAPI (blue). f) 2P and fluorescent IHC images of the colon following the administration of luminal dextran (green) and DAPI (blue) in dtom[iMath1] mice treated with RU486 and antibiotics demonstrating dextran (green) colocalizing with Math1 expressing epithelial cells with GC morphology (red). g and h) 2P images of the colon and i) number of GAPs per crypt from untreated SPF housed mice and antibiotic treated SPF housed mice given vehicle, cholinergic agonists, non-specific or specific mAChR antagonists, or cholera toxin. White arrows denote GAPs, yellow arrows denote the colonic crypt lumen. Data is presented as the mean +/− SEM, * = $p<0.05$, ND = not detected, ns = not significant, n = 3 or more mice for each condition in panels a–d, and g–i, n = 2 in panels e and f, scale bar = 50μm, unless otherwise noted.
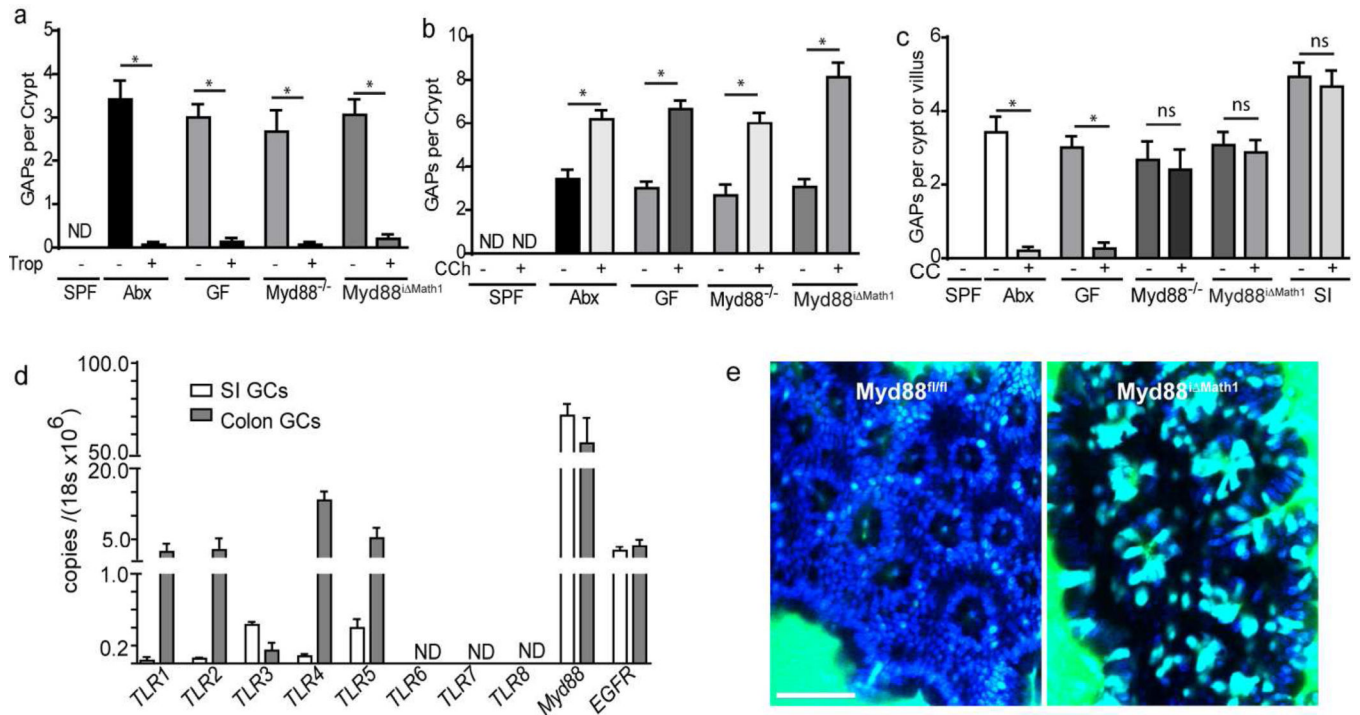
Figure 2. GC intrinsic Myd88-dependent microbial sensing inhibits GAPs in the colon, but not the SI

a–c) Number of GAPs per colonic crypt or SI villus from SPF housed mice, mice treated with antibiotics, germfree (GF) mice, MyD88$^{-/-}$ mice, and Myd88$^{i\Delta Math1}$ mice treated with RU486 given a) tropicamide (Trop), b) carbamylcholine (CCh), or c) luminal heat killed cecal contents from an SPF housed mouse (CC). d) Quantitative real time PCR for the mRNA expression of TLRs, Myd88, and the epidermal growth factor receptor (EGFR) from FACS sorted SI or colonic goblet cells isolated from SPF housed mice. e) 2P images from Myd88$^{i\Delta Math1}$ mice or Myd88$^{fl/fl}$ littermates treated with RU486. Data is presented as the mean +/− SEM, * = p<0.05, ND = not detected, ns = not significant, n = 4 or more mice for each condition in panels a–d, panel e is representative of one of three mice from each condition, scale bar = 50μm.
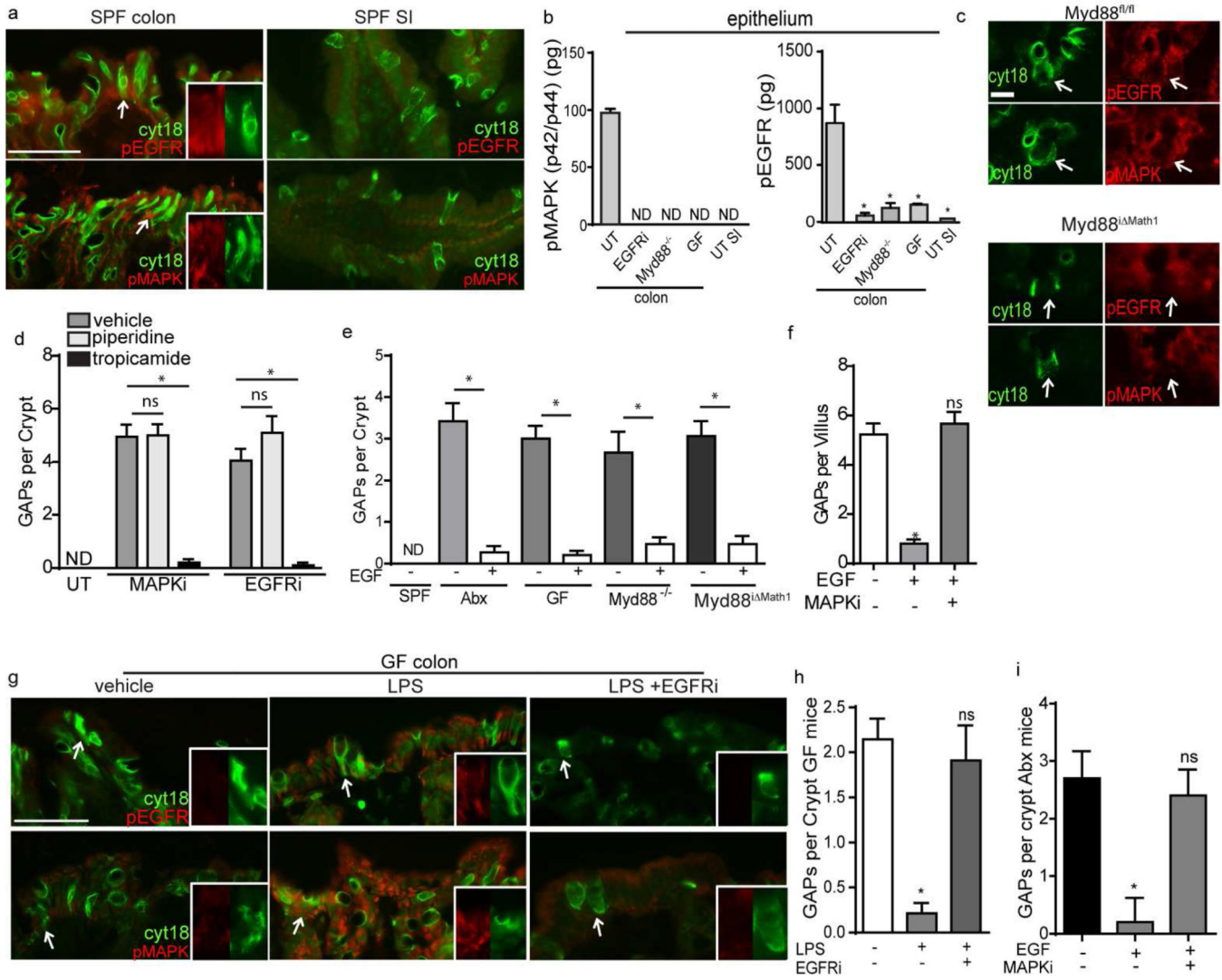
Figure 3. GC intrinsic microbial sensing activates the EGFR, p42/p44 mitogen activated protein kinase (MAPK), and suppresses mAChR$_4$ dependent GAP formation

a) Immunofluorescence staining for phosphorylated EGFR (pEGFR; red), phosphorylated p42/p44 MAPK (pMAPK; red), and cytokeratin 18 (cyt18; green) in the SI and colon of SPF housed mice. White arrow denotes GCs enlarged in inserts with individual channels. b) ELISAs for pMAPK and pEGFR on isolated SI and colonic epithelium from untreated mice (UT), mice treated with an EGFR inhibitor (EGFRi), Myd88$^{-/-}$ mice, and GF mice. c) Immunofluorescence for cyt18, pEGFR and pMAPK in the colon of Myd88$^{i\Delta Math1}$ mice and littermate controls treated with RU486. White arrow indicates the location of a cyt18+ cell in each panel. d) Number of colonic GAPs per crypt in mice treated with EGFRi or MAPKi and antagonists for mAChR$_3$ and mAChR$_4$. e) Number of colonic GAPs per crypt from SPF housed mice with or without antibiotic treatment, GF mice, MyD88$^{-/-}$ mice, and Myd88$^{i\Delta Math1}$ mice treated with RU486 and given vehicle or luminal EGF. f) Number of SI GAPs per villus in SPF housed mice treated with EGF and MAPKi. g) Immunofluorescence for cyt18 (green), pEGFR (red), and pMAPK (red) in the colon of GF mice following intraluminal vehicle (left panel), LPS (middle panel), or LPS and i.p. EGFRi treatment (right

panel). White arrows denotes GCs enlarged in insets with individual channels. h) Number of GAPs per crypt from the colon of GF mice treated with LPS with and without EGFRi treatment. i) Number of GAPs per crypt from the colon of antibiotic treated mice given EGF with and without MAPKi treatment. Data is presented as the mean +/−SEM, * = p<0.05, ND = not detected, ns = not significant, n = 3 or more mice for each condition in panels a, b, and d–i, panel c representative of one of two mice for each condition, scale bar = 20μm in panels a and g; scale bar = 5 μm in panel c.
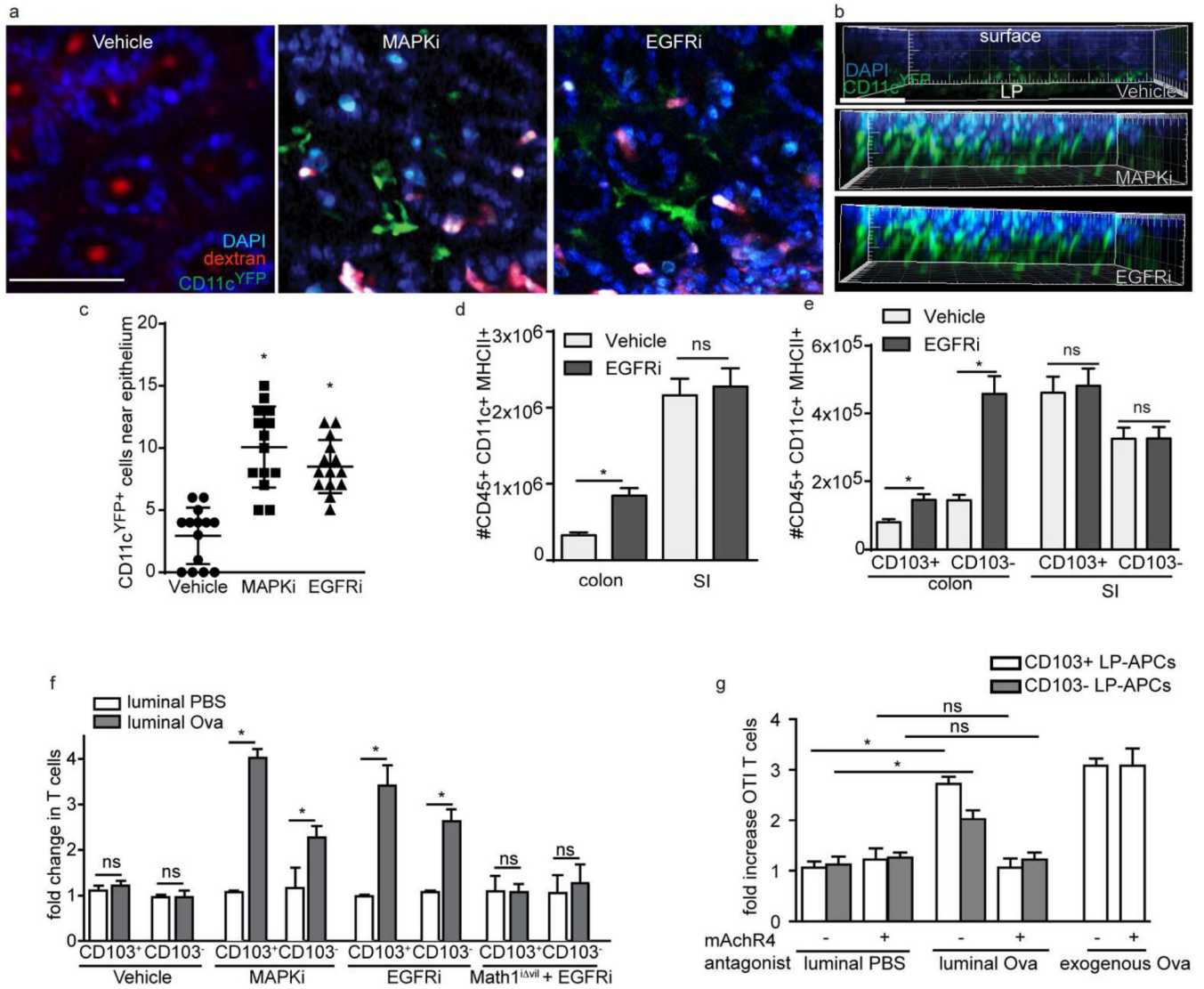
Figure 4. Antigen Presenting Cells (APCs) are recruited to the colonic epithelium and acquire luminal antigen in a mAChR$_4$ dependent manner when GAPs are present

a) 2P images of the colon 20μm below the surface following the administration of luminal dextran (red) and DAPI (blue) in SPF housed CD11c^{YFP} reporter (green) mice treated 24 hours earlier with vehicle (left panel), MAPKi (middle panel) or EGFRi (right panel) b) 3D reconstruction of Z-stacks from the treatment groups with red channel removed to better identify CD11c^{YFP+} cells (major ticks = 20μm). c) The number of CD11c^{YFP+} cells in each group in a volume of 250μm(x) × 220μm(y) × 20μm(z) obtained from the colonic epithelial surface extending into the LP in the z-plane. d) Number of CD11c$^+$MHCII$^+$ LP cells and e) CD103+ and CD103- CD11c$^+$MHCII$^+$ LP cells in the colon and SI 24 hours following treatment with vehicle or EGFRi as assessed by flow cytometry. f and g) Luminal antigen acquisition and presentation capacity of colonic CD103$^+$ and CD103$^-$ LP-APCs isolated from f) vehicle treated, MAPKi treated, or EGFRi treated SPF housed mice or EGFRi treated GC depleted Math1$^{i~vil}$ mice or isolated from g) SPF housed mice treated with EGFRi and mAChR$_4$ antagonists following the administration of luminal PBS or Ova.

Luminal antigen acquisition and presentation capacity was assessed by the expansion of Ova specific OTI T cells following 72 hours of culture. Data is presented as the mean +/− SEM, * = p<0.05, ND = not detected, ns = not significant, n = 3 or more mice for each condition in panels a–e, data in panels f and g are representative of one of three replicates generated by pooling LP-APCs from two mice in each group, scale bar = 50μm.
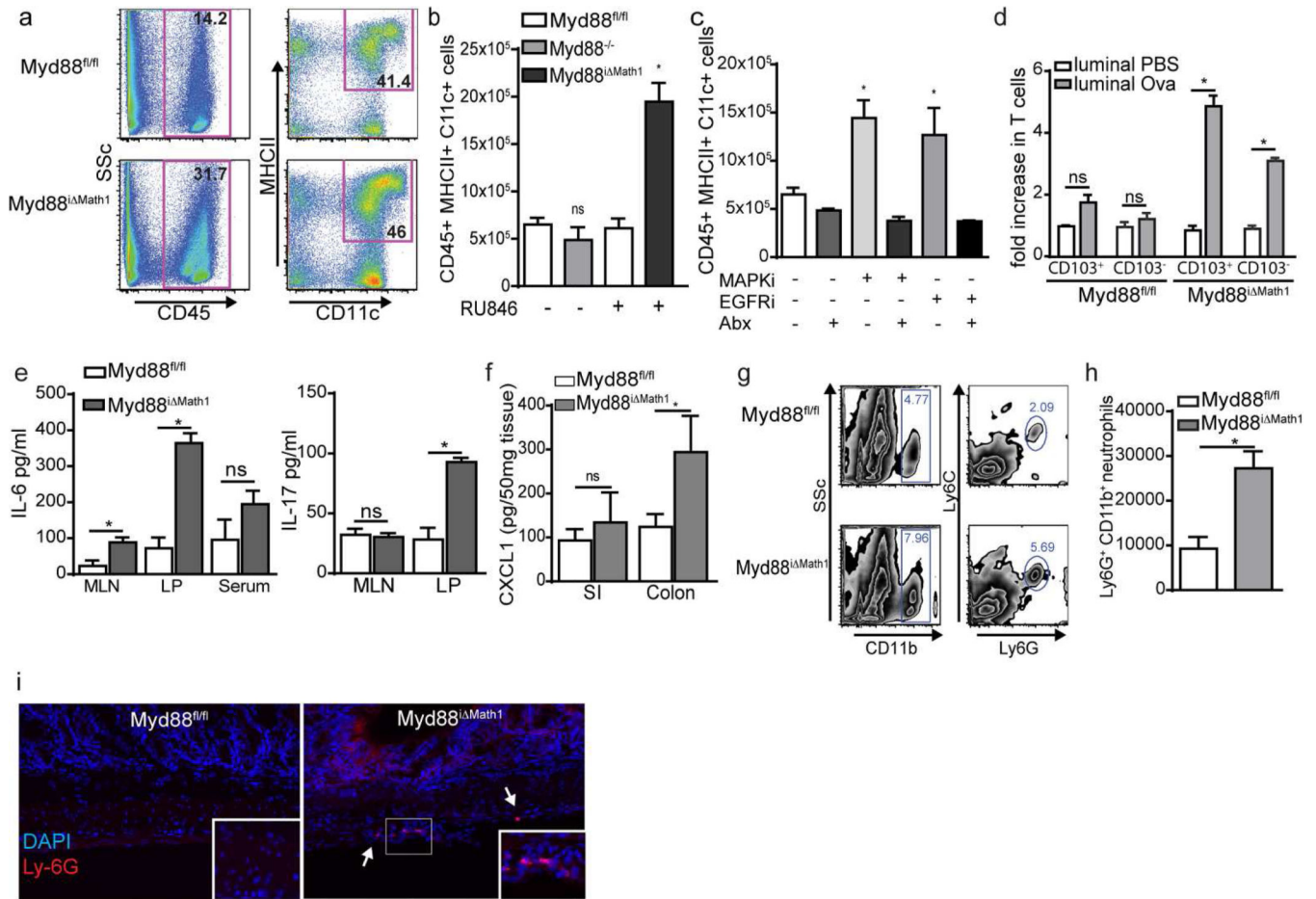
Figure 5. Overriding GC intrinsic microbial sensing and opening colonic GAPs results in an influx of leukocytes and inflammatory cytokine production in response to a non-pathogenic commensal microbiota

a) Representative flow plots of CD45+CD11c+MHCII+ cells in Myd88[i ΔMath1] mice and Myd88^{fl/fl} littermates treated with RU486. b and c) Number of CD45+CD11c+MHCII+ LP cells as assessed by flow cytometry in b) Myd88^{−/−} mice, and Myd88[i ΔMath1] mice and Myd88^{fl/fl} littermates treated with RU486 or c) SPF housed C57BL/6 mice treated with or without antibiotics and MAPKi or EGFRi. d) Luminal antigen acquisition and presentation capacity of colonic CD103^{+} and CD103^{−} LP-APCs isolated from Myd88[i ΔMath1] mice and Myd88^{fl/fl} littermates treated with RU486 following luminal PBS or Ova as assessed by the expansion of Ova specific OTI T cells following 72 hours of culture. e) IL-6 (left panel) and IL-17 (right panel) levels in the serum and culture supernatants from mesenteric lymph node (MLN) or colonic LP cells and f) CXCL1 levels in SI or colon tissue homogenates from Myd88[i ΔMath1] mice and Myd88^{fl/fl} littermates treated with RU486 for four days. g) Representative flow plots, h) number of CD11b^{+}Ly6G^{+} cells in colon, and i) immunofluorescence images Ly6G+ cells in the colon of Myd88[i ΔMath1] mice and Myd88^{fl/fl} littermates treated with RU486 for four days. Data is presented as the mean +/− SEM, * = p<0.05, ND = not detected, ns = not significant, n = 3 or more mice for each condition. scale bar = 50μm.